A mammalian fatty acid hydroxylase responsible for the formation of α-hydroxylated galactosylceramide in myelin

Matthias ECKHARDT[1], Afshin YAGHOOTFAM, Simon N. FEWOU, Inge ZÖLLER and Volkmar GIESELMANN

Institut für Physiologische Chemie, Rheinische-Friedrich-Wilhelms Universität Bonn, Nussallee 11, 53115 Bonn, Germany

Hydroxylation is an abundant modification of the ceramides in brain, skin, intestinal tract and kidney. Hydroxylation occurs at the sphingosine base at C-4 or within the amide-linked fatty acid. In myelin, hydroxylation of ceramide is exclusively found at the α-C atom of the fatty acid moiety. α-Hydroxylated cerebrosides are the most abundant lipids in the myelin sheath. The functional role of this modification, however, is not known. On the basis of sequence similarity to a yeast C_{26} fatty acid hydroxylase, we have identified a murine cDNA encoding FA2H (fatty acid 2-hydroxylase). Transfection of FA2H cDNA in CHO cells (Chinese-hamster ovary cells) led to the formation of α-hydroxylated fatty acid containing hexosylceramide. An EGFP (enhanced green fluorescent protein)–FA2H fusion protein co-localized with calnexin, indicating that the enzyme resides in the endoplasmic reticulum. FA2H is expressed in brain, stomach, skin, kidney and testis, i.e. in tissues known to synthesize fatty acid α-hydroxylated sphingolipids. The time course of its expression in brain closely follows the expression of myelin-specific genes, reaching a maximum at 2–3 weeks of age. This is in agreement with the reported time course of fatty acid α-hydroxylase activity in the developing brain. *In situ* hybridization of brain sections showed expression of FA2H in the white matter. Our results thus strongly suggest that FA2H is the enzyme responsible for the formation of α-hydroxylated ceramide in oligodendrocytes of the mammalian brain. Its further characterization will provide insight into the functional role of α-hydroxylation modification in myelin, skin and other organs.

Key words: ceramide, galactosylceramide, α-hydroxylase, myelin, Scs7p protein, sphingolipid.

INTRODUCTION

Sphingolipids are important components of eukaryotic membranes. They are involved in many cellular functions such as signal transduction, cell–cell interactions and protein sorting [1–3]. Together with cholesterol, sphingolipids are essential for the formation of membrane microdomains or lipid rafts that originate in the Golgi apparatus [4]. The synthesis of sphingolipids starts in the ER (endoplasmic reticulum) with the condensation of palmitoyl-CoA and serine to form 3-oxosphinganine, which is then reduced to sphinganine. Sphinganine is acylated to form dihydroceramide, which is further modified by desaturation and hydroxylation of the sphingosine and fatty acid moiety [5]. The physiological role of the sphingosine and fatty acid hydroxylation is mostly unknown.

In myelin of the mammalian brain, more than 50 % of the cerebrosides contain α-hydroxylated fatty acids. α-Hydroxylation is generated by an NAD(P)H- and O_2-dependent mechanism in the microsomal fraction [6,7]. α-Hydroxylation of sphingolipids has been implicated in the stability of the myelin sheath by offering additional binding sites for ions or hydrogen bonds [8,9]. There is, however, no direct experimental evidence for a functional role of sphingolipid α-hydroxylation in the formation or maintenance of the myelin sheath.

HFA (hydroxy fatty acid)-sphingolipids are also abundant in the skin, kidney, stomach and intestines [10–12]. In addition to α-hydroxylated sphingolipids, these tissues synthesize 4-hydroxysphinganine (phytosphingosine)-containing sphingolipids. It has been suggested that the additional hydroxy group increases the rigidity of intercellular lipid aggregates, which is important to build up an efficient water barrier of the skin [5]. Support for this hypothesis comes from recent observations in mice lacking the transcription factor Arnt [13]. In these mice, a significant decrease in 4- and α-hydroxy sphingolipids correlates with a functional breakdown of the water barrier function of the skin. Decreased 4-hydroxysphinganine levels have also been observed in psoriasis, which is characterized by deficits in the skin barrier function [14].

In *Saccharomyces cerevisiae*, the formation of the α-hydroxylated C_{26} fatty acid containing IPC (inositolphosphoceramide) requires the Scs7p protein, which belongs to the family of desaturases/hydroxylases [15,16]. Scs7p hydroxylates the fatty acid moiety, most probably on the level of dihydroceramide [16]. A BLAST search using Scs7p as the query enabled us to identify the EST (expressed sequence tag) and cDNA sequences potentially encoding mammalian α-hydroxylases. In the present study, we describe the identification and functional expression of a murine FA2H (fatty acid 2-hydroxylase) required for the formation of hydroxylated sphingolipids in myelin, kidney, skin and the intestinal tract.

EXPERIMENTAL

Cloning of FA2H cDNA

To identify potential mammalian fatty acid α-hydroxylases, a BLAST search was performed with the *S. cerevisiae* C_{26} fatty acid

Abbreviations used: CGT, UDP-galactose:ceramide galactosyltransferase; CHO cells, Chinese-hamster ovary cells; DIG, digoxigenin; EGFP, enhanced green fluorescent protein; ER, endoplasmic reticulum; EST, expressed sequence tag; FA2H, fatty acid 2-hydroxylase; GalC, galactosylceramide; HexC, monohexosylceramide; HFA, hydroxy fatty acid; HFAME, HFA methyl ester; IPC, inositolphosphoceramide; MALDI–TOF, matrix-assisted laser-desorption ionization–time-of-flight; NFA, non-HFA; ORF, open reading frame; PLP, proteolipid protein; VLCFA, very-long-chain fatty acid.

[1] To whom correspondence should be addressed (email eckhardt@institut.physiochem.uni-bonn.de).

The nucleotide sequence data reported will appear in DDBJ, EMBL, GenBank® and GSDB Nucleotide Sequence Databases under the accession number AY660882.

IPC hydroxylase Scs7p [15] as the query. Several EST and cDNA sequences of murine and human origin as well as other species were found. The IMAGE consortium cDNA clone IMAGp998-B1814017Q (6476561; obtained from RZPD Deutsches Ressourcenzentrum für Genomforschung, Berlin, Germany) contains the putative start codon of FA2H, and sequencing revealed that the complete ORF (open reading frame) was present. However, we found a deletion of two nucleotides (nt 99 and 100 of the coding region) within the ORF, but this deletion was not present in most other cDNA and EST sequences in the database. This deletion was corrected by site-directed mutagenesis as described in [17] using mutagenic oligonucleotides FA2H-CT1 (5′-CCGCGGGGCCAGCCTCTACGACCTCACCAGC-3′) and FA2H-CT2 (5′-GCTGGTGAGGTCGTAGAGGCTGGCCCCG-CGG-3′) and FA2H in pCMV-SPORT6 as template. The coding region and the 3′-non-coding sequence of FA2H were amplified by PCR using the oligonucleotides FA2H-sense (5′-GCAAGC-TTAGCTCCGCTCTCCCGCCATGG-3′) and T7 (5′-TCTAATA-CGACTCACTATAGGG-3′). The PCR product was digested with HindIII and XbaI and subcloned into the pcDNA3.1/zeo(+) vector (Invitrogen, Karlsruhe, Germany), resulting in the plasmid pcDNA3.1/zeo/FA2H. An FA2H fusion protein with N-terminal EGFP (enhanced green fluorescent protein) was generated by digesting pcDNA3.1/zeo/FA2H with NcoI and XbaI, which deliberates the FA2H cDNA. After a fill-in reaction with the Klenow enzyme, the FA2H cDNA was subcloned into the SmaI site of the pEGFP-C1 plasmid (Clontech, Heidelberg, Germany), resulting in the plasmid pEGFP-FA2H. The identity of all constructs generated were confirmed by DNA sequencing.

Sequence analysis

FA2H sequences from mouse, human, drosophila, *Caenorhabditis elegans* and *S. cerevisiae* were aligned using DNAStar and the alignment was further edited using the BOXSHADE program (at http://ulrec3.uni.ch/software/BOX_form.html). Putative transmembrane domains were predicted using the TMHMM program ([18]; at http://www.cbs.dtu.dk/services/TMHMM/). Hydrophobicity plots were generated by the method of Kyte and Doolittle [19] with a window size of 17 amino acids (at http://bioinformatics.weizmann.ac.il/).

Northern-blot analysis

Total RNA of different murine tissues was isolated using acid phenol method as described in [20] or using TRIzol® (Invitrogen) according to the manufacturer's instructions. Total RNAs (20 μg/lane) were separated in 1 M formaldehyde/1 % agarose gels and transferred on to positively charged Hybond-N$^+$ nylon membranes (Amersham Biosciences, Freiburg, Germany). A 1.4 kb HindIII fragment of the FA2H cDNA and a 1.5 kb actin fragment (Stratagene, Heidelberg, Germany) were used as probes, which were prepared using the Megaprime DNA Labelling System and cytidine 5′-[α-^{32}P]triphosphate (Amersham Biosciences). Hybridization was performed using standard procedures [20]. Radioactive signals were detected by autoradiography on X-ray films. Quantification was performed by phosphoimaging using a Bio-Imaging Analyzer BAS-1800II (Fuji Photo Film, Düsseldorf, Germany) and AIDA software (Raytest, Straubenhardt, Germany).

Transfection

CHO (Chinese-hamster ovary)-CGT (UDP-galactose:ceramide galactosyltransferase) cells (kindly provided by B. Popko, University of Chicago) were maintained in DMEM (Dulbecco's modified Eagle's medium)/Nut Mix F12 (1:1, v/v), supplemented with 5 % (v/v) fetal calf serum, 2 mM glutamine, 100 units/ml penicillin and 100 μg/ml streptomycin (all from Invitrogen). A total of 1 million CHO-CGT cells were seeded into 10 cm dishes and transfected using the appropriate plasmid (4 μg) and 24 μl of Lipofectamine™ (Invitrogen) in OptiMEM medium (Invitrogen). For this purpose, cells were washed twice with PBS, then 3.6 ml of OptiMEM medium was added, followed by 24 μl of Lipofectamine™ in 200 μl of OptiMEM and 4 μg of plasmid diluted in 200 μl of OptiMEM. Transfections were stopped after 12–16 h by changing the medium to normal growth medium containing 5 % fetal calf serum. To generate stably transfected CHO-CGT cells expressing FA2H, cells were transfected with the plasmid pcDNA3.1/zeo/FA2H and stably transfected cells were selected using 400 μg/ml zeocin.

Immunofluorescence

Cells were trypsinized 24 h after transfection and then seeded at an appropriate density on to glass coverslips. After another 24 h, cells were fixed in 4 % (w/v) paraformaldehyde in PBS and processed for indirect immunofluorescence as follows. Cells were permeabilized with 0.3 % Triton X-100 in PBS for 10 min, followed by blocking non-specific binding in 0.2 % gelatin in PBS (overnight at 4 °C). Thereafter, rabbit anti-calnexin (Stressgen/Biomol, Hamburg, Germany) in 0.2 % gelatin/PBS was applied for 2 h. After washing with PBS, Cy3-conjugated goat anti-rabbit Ig (Jackson Immunoresearch Laboratories, West Grove, PA, U.S.A.) was used to detect primary antibodies. Nuclei were stained with Hoechst dye H33258 (Sigma, Taufkirchen, Germany).

Western-blot analysis

Western-blot analysis was performed as described in [17]. Cells were lysed in 20 mM Tris/HCl (pH 8.0), 150 mM NaCl, 1 % Triton X-100, 5 mM EDTA and 1 mM PMSF. Protein concentration was determined using the Bio-Rad DC protein assay. Samples of EGFP or EGFP–FA2H-transfected CHO-CGT cells were separated by SDS/PAGE (10 % polyacrylamide) and blotted on to nitrocellulose membranes using the semi-dry blotting technique. Bound EGFP proteins were detected using anti-GFP antibody (Abcam, Cambridge, U.K.) and peroxidase-labelled anti-rabbit Ig (Dianova, Hamburg, Germany). The bound antibodies were visualized using chemiluminescence. For this purpose, membranes were incubated for 1 min in 2.7 mM H_2O_2, 1.25 mM 3-aminophthalhydrazide, 0.2 mM *p*-coumaric acid and 100 mM Tris/HCl (pH 8.5) and exposed to X-ray films.

Lipid extraction and TLC

Lipids were isolated from transfected CHO cells as described by van Echten-Deckert [21] with minor modifications. Briefly, cells were scraped in methanol. Then, 2 vol. of chloroform was added and lipids were extracted for 2 h at 50 °C with constant stirring. The insoluble material was removed by filtration through glass wool and lipids were dried at 45 °C under a stream of nitrogen. Desalting and alkaline hydrolysis were performed as described in [21]. Lipids were dissolved in chloroform/methanol (1:1, v/v) and stored at −20 °C. Lipids were separated on silica gel 60 TLC or HPTLC silica gel plates (Merck, Darmstadt, Germany) using the solvent system chloroform/methanol/water (35:15:2, by vol.). Lipids were visualized by spraying with 0.625 M copper sulphate in 8 % (v/v) phosphoric acid [22], followed by heating for

15–20 min at 150 °C. GalC (galactosylceramide) and sulphatide from bovine brain (Sigma) were used as standards.

Acid methanolysis of sphingolipids

Total alkali-stable lipids or TLC-purified GalC were subjected to acid methanolysis. Lipids were incubated in 32 % HCl/methanol/water (3:29:4, by vol.) at 78 °C for 16–18 h [15,23]. Thereafter, fatty acid methyl esters were isolated by extracting twice with n-hexane. The hexane extracts were combined, dried under nitrogen, dissolved in n-hexane and separated by TLC using light petroleum (boiling range 40–60 °C)/diethyl ether (17:3, v/v) as the solvent system. Fatty acid methyl esters were visualized as described above. Acid methanolysis products of GalC from bovine brain containing NFA-GalC (where NFA stands for non-HFA) and HFA-GalC (Sigma) and [*stearoyl*-$^2H_{35}$]*N*-stearoylpsychosine (cerebroside with a $C_{18}{}^2H_{35}$ fatty acid side chain) '*N*-stearoyl-d35-psychosine'; Matreya, Pleasant Gap, PA, U.S.A.) served as reference substances.

MALDI–TOF-MS (matrix-assisted laser-desorption ionization–time-of-flight MS)

Regions containing the lipid of interest were cut out from TLC plates and extracted with chloroform/methanol (1:1, v/v), dried under nitrogen and dissolved in chloroform/methanol (1:1, v/v). Then, 1 μl of the sample was mixed with 1 μl of 2,5-dihydroxybenzoic acid (10 mg/ml in 70 %, v/v, acetonitrile); 1 μl of the mixture was loaded into a well of a 100-well sample plate. Mass spectra were recorded with a Voyager-DE STR mass spectrometer (PE Biosystems, Warrington, Cheshire, U.K.) in positive-ion mode (instrument settings were 25 000 V accelerating voltage and 75 % grid voltage). [*stearoyl*-$^2H_{35}$]*N*-stearoylpsychosine served as the reference substance.

In situ hybridization

Antisense and sense DIG-11-UTP-labelled RNA probes (where DIG stands for digoxigenin) of the FA2H and PLP (proteolipid protein) cDNAs were synthesized using SP6, T3 or T7 RNA polymerase (Roche Diagnostics, Mannheim, Germany) according to the manufacturer's instructions. Mice (CBA × C57BL/6 genetic background) were perfused through the left cardiac ventricle with 4 % paraformaldehyde in PBS. Brains were removed and post-fixed in 4 % paraformaldehyde in PBS. Brains were dehydrated, paraffin-embedded and cut at a thickness of 8 μm using a microtome (Leica HM 355 S; Leica, Lasertechnik, Heidelberg, Germany). Hybridizations were performed as described by Baader et al. [24]. Briefly, after deparaffination, sections were post-fixed in 4 % paraformaldehyde in PBS. Endogenous peroxidases were inhibited by incubation with 1 % H_2O_2/PBS for 15 min. Thereafter, sections were treated with proteinase K (10 μg/ml; 4 min) and permeabilized with 0.25 % Triton X-100 (4 min). Specimens were then incubated with 0.2 M HCl (8 min), followed by 0.1 M triethanolamine/2.5 μl/ml acetic anhydride (10 min). The sections were washed once for 10 min with 2 × SSC (0.15 M NaCl/0.015 M sodium citrate) at 50 °C and hybridized to DIG probes overnight at 70 °C in 50 % (v/v) formamide, 1 % Denhardt's solution, 0.2 % SDS, 0.25 mg/ml salmon sperm DNA, 0.25 mg/ml yeast tRNA and 10 % (w/v) hybridization salt (3 M NaCl, 0.1 M Pipes and 0.1 M EDTA). Sections were washed with 2 × SSC at 60 °C, for 20 min with 50 % formamide/1 × SSC at 60 °C and for 45 min with 0.1 × SSC at 70 °C. DIG probes were detected by incubation with alkaline phosphatase-conjugated anti-DIG F_{ab} fragment (Roche Diagnostics). Bound antibodies were visualized using Nitro Blue Tetrazolium and 5-bromo-4-chloro-3-indolyl phosphate (Merck) in 100 mM Tris/HCl (pH 9.5), 100 mM NaCl and 50 mM $MgCl_2$.

RESULTS

A BLAST search using the Scs7p of *S. cerevisiae* [15] as the query resulted in the identification of several mammalian cDNA and EST sequences having significant similarity to the yeast enzyme. A cDNA clone harbouring the complete ORF was generated as described in the Experimental section. The gene was named FA2H (GenBank® accession no. AY660882). The murine gene is composed of seven exons spanning approx. 50 kb on chromosome 8 (according to the NCBI map viewer at http://www.ncbi.nlm.nih.gov/mapview/). The ORF of 1119 nt potentially encodes a protein of 372 amino acids with a calculated molecular mass of 43 kDa (Figure 1A). Comparison of different murine EST sequences in the databases revealed that FVB/N and C57BL/6J mice differ at three nucleotide positions [C308T, T1044G and T1061C], leading to three amino acid exchanges (T103I, F348L and L354P). Interestingly, two of them (F348L and L354P) affect conserved motifs at the C-terminus. The cDNA analysed in the present study was derived from FVB/N mice.

The encoded protein contains an N-terminal cytochrome b_5 domain and four conserved histidine-containing $HX_{(2-3)}(XH)H$ motifs (h1–h4; Figures 1A and 1C). The histidine motifs are characteristic of the family of membrane-bound lipid desaturases/hydroxylases [25,26]. These motifs probably form oxo-di-iron centres, which transfer electrons from the cytochrome b_5 domain to the substrate [27]. Hydrophobicity plots (Figure 1B) indicated that the protein contains several hydrophobic regions, and the TMHMM algorithm [17] predicted four transmembrane regions (Figure 1C). Interestingly, one of the histidine motifs (h3) is within the predicted transmembrane domain TM4 of the murine, human and *Drosophila* protein. For the *C. elegans* and *S. cerevisiae* sequences, however, this motif lies in the cytosolic part close to the membrane region.

To examine whether FA2H encodes a functional FA2H, we used CHO-CGT cells, which are stably transfected with CGT [28]. CHO cells do not express α-hydroxylase activity [29]. We decided to use CHO-CGT instead of wild-type CHO cells since CGT has a high affinity for HFA-ceramide [29] and GalC is not converted into more complex glycolipids. The FA2H cDNA ORF was subcloned into the expression vector pcDNA3.1/zeo and transfected transiently and stably into CHO-CGT cells. Either cells transfected with pEGFP-C1 plasmid or mock-transfected cells served as the controls. After 48 h, lipids were extracted from transfected cells, subjected to alkaline hydrolysis to remove phospholipids and analysed by TLC as shown in Figure 2(A). Compared with control cells (EGFP- or mock-transfected), there was a clear increase in HexC (monohexosylceramide) species co-migrating with the HFA-GalC standard in FA2H-transfected cells, suggesting the formation of HFA-GalC.

To verify the synthesis of hydroxylated fatty acids, the sphingolipids were subjected to acid hydrolysis and the generated fatty acid methyl esters were separated by TLC (Figure 2B). Whereas HFAMEs (HFA methyl esters) were hardly detectable in mock-transfected cells or in cells transiently transfected with the pEGFP-C1 vector, HFAME could easily be detected in FA2H-transfected cells. These results strongly suggest that FA2H-expressing CHO-CGT cells attained the ability to synthesize HFA-containing cerebrosides.

To confirm these results by an independent method and to evaluate the structure of the lipids in more detail, the sphingolipids co-migrating with GalC were isolated from the TLC plate,

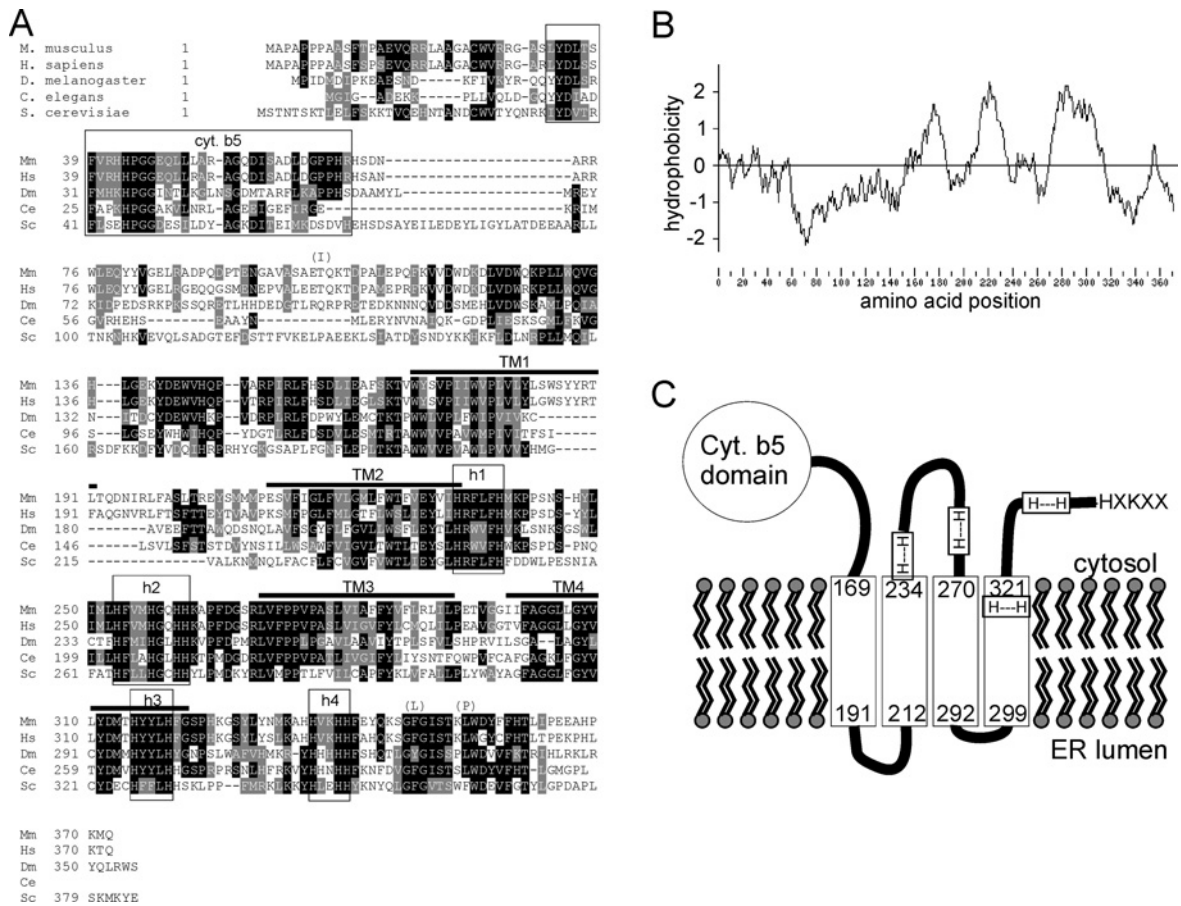

Figure 1 Sequence and structure prediction of murine FA2H

(**A**) Sequence alignment of FA2H from *Mus musculus* (Mm; FVB/N strain; GenBank® accession no. AY660882), *Homo sapiens* (Hs; GenBank® accession no. AAH04263), *Drosophila melanogaster* (Dm; GenBank® accession no. AAL68319), *Caenorhabditis elegans* (Ce; GenBank® accession no. NP_492678) and *S. cerevisiae* (Sc; GenBank® accession no. NP_013999). The conserved cytochrome b_5 (cyt. b5) and the four histidine motifs (h1–h4) are boxed. Potential transmembrane domains were predicted using the TMHMM program and are indicated by black bars on top of the mouse sequence. Note that the amino acid sequence of C57BL/6J mice (GenBank® accession no. NP_835187) differs at three positions from that of FVB/N mice. The amino acids found in C57BL/6J mice are shown on top of the mouse sequence. Similarities between the sequences were highlighted using the BOXSHADE program. (**B**) Hydrophobicity plot of murine FA2H generated by the method of Kyte and Doolittle [19] using a window size of 17 amino acids. (**C**) Membrane topology model of FA2H. The numbers of the first and last amino acids of each transmembrane domain are indicated. The four conserved histidine motifs are indicated by 'H—H'. Note that, according to the TMHMM prediction, the histidine motif h3 might be located within the fourth transmembrane domain. A potential ER retention signal motif (HXKXX) is present at the C-terminus of FA2H.

re-extracted with chloroform/methanol (1:1, v/v) and analysed by MALDI–TOF-MS (Figure 3). In mock- (Figure 3A) or EGFP-transfected (results not shown) cells, ions with *m/z* values of 722, 806 and 834 for $[M + \mathrm{Na}]^+$ could be detected. These mass peaks correspond to non-hydroxylated HexC species containing sphingosine with C_{16}, C_{22} and C_{24} fatty acids respectively. In FA2H-transfected cells, additional ion peaks were observed at *m/z* 738, 822 and 850, indicative of hydroxylation (+16 Da; Figure 3B).

α-Hydroxylase activity has been observed in the microsomal fraction of rat brains [7]. Therefore, and because of the synthesis of ceramide and HFA-GalC in the ER [31], it was reasonable to assume that the FA2H enzyme resides in the ER. In concordance with this, the FA2H C-terminus contains a putative ER retention signal (-HXKXX; see Figures 1A and 1C). To determine the subcellular localization of the FA2H protein, we generated the expression plasmid pEGFP-FA2H, which codes for the fusion protein of FA2H with an N-terminal EGFP. CHO-CGT cells were transiently transfected with pEGFP-FA2H (Figures 4A, 4C and 4E) or the empty vector pEGFP-C1 (Figures 4B, 4D and 4F) and stained with an antibody directed against the ER marker calnexin. A high degree of co-localization of the EGFP–FA2H fusion protein with calnexin was evident (Figures 4A and 4C). To confirm that the EGFP–FA2H was active, sphingolipids were extracted from EGFP–FA2H and control EGFP-transfected cells and analysed by MALDI–TOF-MS as described above. The mass spectra obtained clearly demonstrated the presence of hydroxylated HexC in EGFP–FA2H-transfected cells (Figure 3C), but not in EGFP control cells (results not shown), indicating that the fusion protein was active. Western-blot analysis of total cell lysates from transiently EGFP–FA2H-transfected cells using an anti-GFP antibody led to the detection of an approx. 70 kDa protein, which is in good agreement with the calculated mass of 71.8 kDa for the fusion protein (Figure 4G).

Northern-blot analysis of total RNA from diverse adult mouse tissues indicated that FA2H is highly expressed in brain, skin, stomach, testis and kidney (Figure 5A). This expression pattern is in agreement with the presence of α-hydroxylated sphingolipids in these tissues [10–12,32]. A very weak signal could be detected in RNA from the small intestine; however, it was too faint to be displayed in Figure 5(A). The size of the mRNA was calculated to be 2.6 kb. In brain, FA2H expression strongly increased between 1 and 2 weeks of age (Figure 5B). Expression

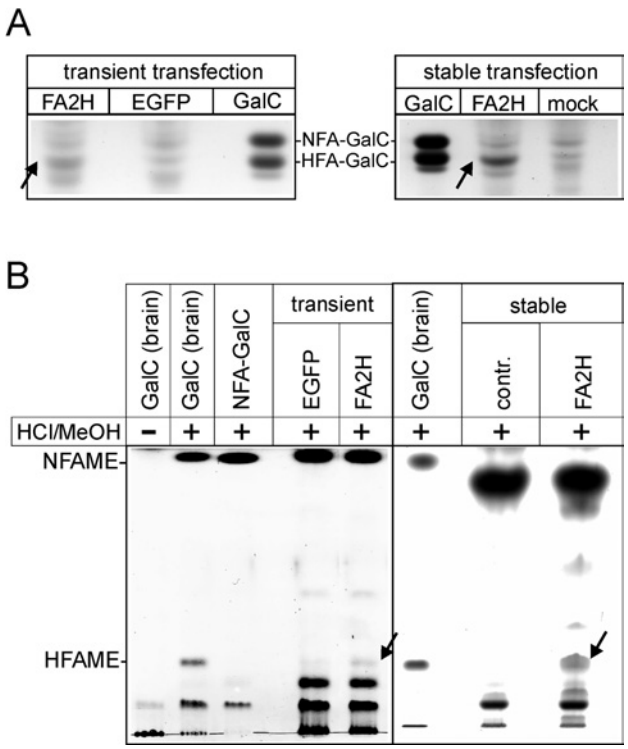

Figure 2 Sphingolipid and fatty acid analysis of FA2H-transfected CHO cells

(**A**) TLC analysis of alkali-stable lipids from CHO-CGT cells transiently or stably transfected with FA2H cDNA in pcDNA3.1/zeo (FA2H), pEGFP-C1 plasmid (EGFP) or mock-transfected cells. The amount of lipids corresponding to 500 μg of protein was applied on silica gel 60 HPTLC plates. GalC from bovine brain served as the reference substance. To visualize lipids, TLC plates were sprayed with 0.625 M copper sulphate in 8 % phosphoric acid and heated for 15 min at 150 °C. An increase in sphingolipids co-migrating with α-hydroxylated fatty acid-containing GalC (HFA-GalC; arrow) appeared in transiently and stably FA2H-transfected cells compared with control (EGFP- or mock-transfected) cells. NFA-GalC, NFA-containing GalC. (**B**) Sphingolipids from CHO-CGT cells transiently or stably transfected with FA2H cDNA in pcDNA3.1/zeo (FA2H), pEGFP-C1 plasmid (EGFP) or untransfected cells (contr.) were subjected to acid methanolysis for 16 h at 78 °C (+), extracted with n-hexane and separated on silica gel 60 HPTLC plates in light petroleum (boiling range 40–60 °C)/diethyl ether (17:3) as the solvent system. GalC from bovine brain [subjected (+) or not (−) to acid methanolysis] and [stearoyl-$^2H_3$]*N*-stearoylpsychosine (NFA-GalC) served as reference substances. Lipids were stained as in (**A**). In EGFP- or mock-transfected cells, HFAMEs were hardly detectable. In contrast, HFAME could be identified in FA2H-transfected cells (arrows). NFAME, NFA methyl ester.

reached the maximal level between 2 and 3 weeks of age and slightly decreased in older animals (Figures 5B and 5C). This profile closely resembles that of myelin-specific genes, such as CGT, myelin basic protein or PLP [30,33,34]. Furthermore, the time course of FA2H mRNA expression in the developing mouse brain is similar to that of α-hydroxylase activity reported by Murad and Kishimoto [35], suggesting that α-hydroxylation is mainly regulated at the transcriptional level.

In situ hybridization of 3-week-old murine brain using a DIG-labelled FA2H antisense RNA probe detected an expression of FA2H in the white matter (Figure 6). Figure 6 shows the hybridization pattern in the cerebellum (Figures 6A and 6D) and forebrain (Figures 6G and 6L). No hybridization signals were obtained with the sense probe (Figures 6B, 6E, 6J and 6M). Hybridization of adjacent sections with an antisense PLP probe (Figures 6C, 6F, 6H and 6N), which is a specific marker for differentiated oligodendrocytes [36], gives a very similar hybridization pattern, confirming that FA2H expression is mainly restricted to oligodendrocytes. Taken together, the above results strongly suggest that FA2H is the hydroxylase responsible for the synthesis of α-hydroxylated GalC in myelinating oligodendrocytes.

DISCUSSION

We have identified murine and human cDNA sequences potentially encoding a fatty acid α-hydroxylase. The protein belongs to the family of membrane-bound lipid desaturases/hydroxylases and the following observations strongly suggest that FA2H is the hydroxylase responsible for the formation of α-hydroxylated cerebrosides and other sphingolipids. First, CHO-CGT cells, which normally do not have hydroxylated HexC [29], synthesize hydroxylated HexC after transfection with an FA2H cDNA. Secondly, FA2H contains four histidine motifs, which is characteristic of the enzyme family of lipid desaturases/hydroxylases [25,26]. Thirdly, FA2H is expressed in those tissues that synthesize α-hydroxylated sphingolipids, and the time course of FA2H expression in brain is similar to that of α-hydroxylase activity reported by Murad and Kishimoto [35]. Since FA2H expression was very low in the small intestine, we cannot rule out that a second enzyme exists that might be involved in α-hydroxylation in the intestinal tract. At least a recent database search did not indicate the presence of a second enzyme with significant sequence similarity to FA2H in the human or mouse genome (M. Eckhardt, unpublished work).

α-Hydroxylase activity in brain microsomes is NAD(P)H- and O_2-dependent [6,7]. Thus probably the N-terminal cytochrome b_5 domain is reduced by NADPH:cytochrome b_5 reductase and then transfers electrons to the oxo-di-iron centres formed by the histidine motifs $HX_{2-3}(XH)H$ (h1–h4; see Figures 1A and 1C). These motifs are found in all enzymes that desaturate or hydroxylate lipids in an NAD(P)H- and O_2-dependent manner [26,27]. For the rat stearoyl-CoA Δ9 desaturase, all histidine residues of the histidine motifs are essential for enzymic activity [37]. Interestingly, most enzymes exhibiting desaturase activity contain only three histidine motifs [26], whereas four histidine motifs are present in the yeast and mammalian sphinganine/dihydroceramide C-4 hydroxylases [16,38] and yeast α-hydroxylase [15,39]. This suggests that the additional histidine motif might be important for the hydroxylase activity. Histidine motifs h1 and h3 are close to or (h3) maybe within transmembrane regions, and thus are ideal candidates for the active centre of the enzyme.

The immediate substrate of the α-hydroxylase has not been definitely identified. Akanuma and Kishimoto [40] suggested that neither ceramide nor the free fatty acid but an unidentified intermediate is the substrate for the α-hydroxylase in brain. In lower eukaryotes, however, there is evidence for direct hydroxylation of ceramide [16,41]. For example, yeast mutants lacking the C-4 hydroxylase Sur2p accumulate non-hydroxylated IPC, suggesting that Scs7p recognizes ceramide and prefers phytosphingosine-containing ceramide rather than non-hydroxylated ceramide as the substrate [16]. In view of the sequence similarity to the yeast enzyme, it is probable that ceramide is the substrate for the FA2H enzyme.

Yeast Scs7p and its *Arabidopsis* homologue are required for the synthesis of VLCFA (C_{26}) ceramide (where VLCFA stands for very-long-chain fatty acid) [15,16,39]. Hydroxylation of C_{16} fatty acid-containing ceramides by Scs7p has not been reported. In contrast, transfection of FA2H into CHO cells resulted in the synthesis of hydroxylated derivatives of all HexC species. An exceptionally high proportion of VLCFA is found in the brain HFA-GalC pool [42]. One important question will be to determine whether the higher proportion of VLCFA in the α-hydroxylated ceramides is due to differences in the substrate affinity of the

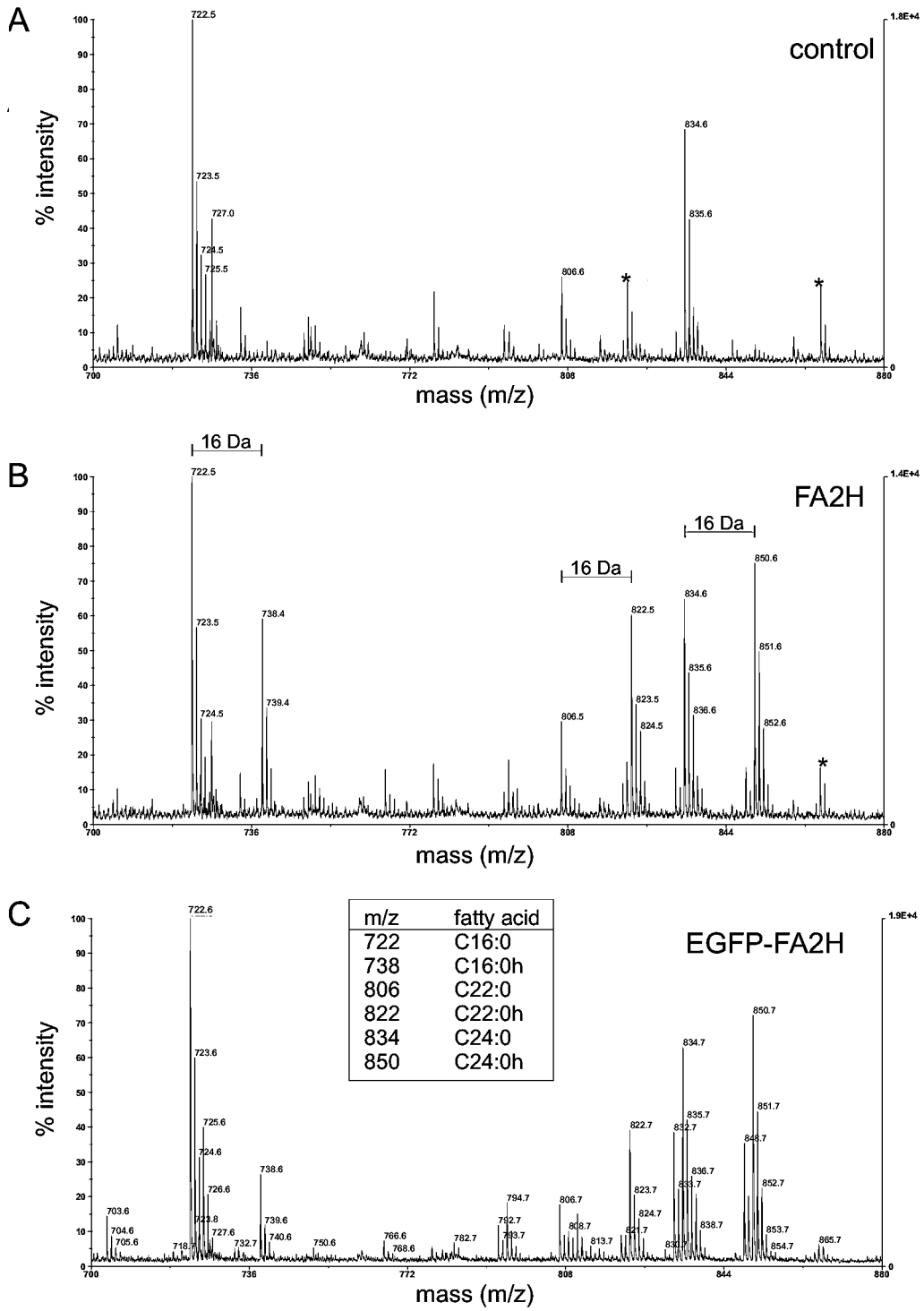

Figure 3 MALDI–TOF-MS of HexCs from FA2H-transfected CHO cells

Sphingolipids of transiently transfected CHO-CGT cells co-migrating with the GalC standard were isolated from TLC plates and analysed by MALDI–TOF-MS in the positive ion mode. In mock-transfected cells (**A**), ion peaks $[M + Na]^+$ at *m/z* 722, 806 and 834 corresponding to HexC with non-hydroxy C_{16}, C_{22} and C_{24} fatty acids (see inset to **C**) could be detected. Similar results were obtained for cells transfected with the pEGFP-C1 plasmid (results not shown). Ion peaks marked by asterisks (*m/z* 821 and 865) are caused by contaminations from the TLC silica gel matrix. Sphingolipids from FA2H- (**B**) or EGFP–FA2H-transfected (**C**) cells gave additional mass ion peaks at *m/z* 738, 822 and 850, indicating the presence of hydroxylated HexC (+16 Da). The measured *m/z* positive molecular ion $[M + Na]^+$ signals assigned to individual molecular HexC species are shown in the inset to (**C**). Note: $1.8E + 4 = 1.8 \times 10^4$ etc.

enzyme or different sorting of short- and long-chain fatty acid-containing ceramides within the ER membrane.

The functional role of sphingolipid hydroxylation and, in particular, α-hydroxylation is largely unknown. Several studies showed that α-hydroxylation affects the binding of sphingolipids to antibodies or toxins [43,44]. Furthermore, the calcium-dependent *trans*-interaction between GalC- and sulphatide-containing membranes is significantly increased when the lipids are

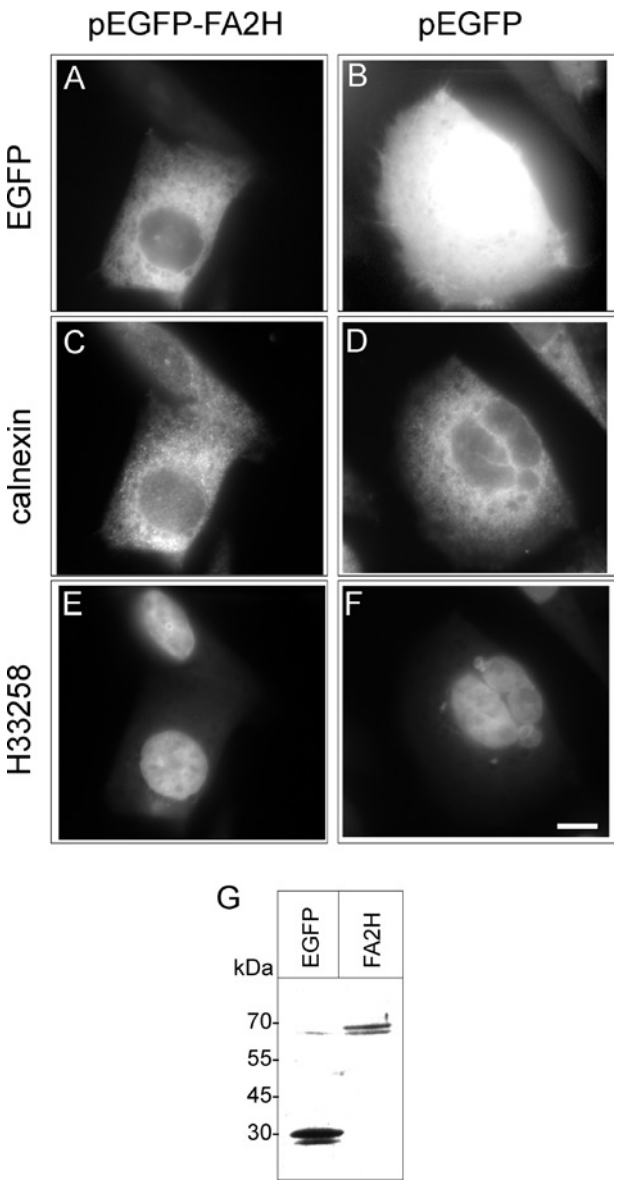

Figure 4 Subcellular localization of EGFP–FA2H fusion protein

CHO-CGT cells were transiently transfected with pEGFP-FA2H (**A**, **C**, **E**) or the empty vector pEGFP-C1 (**B**, **D**, **F**); 2 days after transfection, cells were fixed in paraformaldehyde and stained for the ER marker calnexin, using a rabbit antiserum and anti-rabbit Ig–Cy3 conjugate as the secondary antibody (**C**, **D**). Nuclei were stained with Hoechst dye H33258 (**E**, **F**). Scale bar, 10 μm. (**G**) Western-blot analysis of CHO-CGT cells transfected with pEGFP-C1 (EGFP) or pEGFP-FA2H (FA2H). Cell lysates (20 μg of EGFP and 40 μg of FA2H) were resolved by SDS/PAGE, transferred on to nitrocellulose and stained with an antiserum directed against GFP. Proteins of approx. 30 kDa (EGFP) and 70 kDa (EGFP–FA2H) respectively were detected, in accordance with the calculated molecular masses. Staining of an approx. 68 kDa protein in both lanes was due to non-specific binding of the primary antibody.

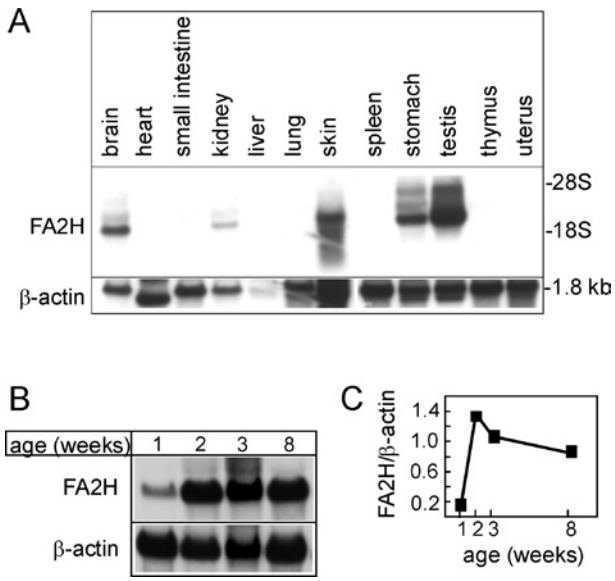

Figure 5 Tissue distribution of FA2H mRNA expression

(**A**) Total RNAs (20 μg/lane) from diverse murine tissues (4 months old) were separated on a 1% agarose/1 M formaldehyde gel. After transferring on to nylon membranes, the RNAs were hybridized to an [α-^{32}P]dCTP-labelled FA2H cDNA probe. The bound probes were visualized by autoradiography. (**B**) Total RNAs (20 μg) from mouse brains of different ages (1, 2, 3 and 8 weeks) were transferred on to a nylon membrane and hybridized to an FA2H cDNA probe. Membranes were rehybridized to an actin-specific cDNA probe. (**C**) Radioactive signals were quantified using a Bioimager. FA2H mRNA levels were normalized to β-actin mRNA and plotted as a function of time.

α-hydroxylated [9,45]. Biophysical studies using artificial membranes suggest that the presence of α-hydroxy groups greatly influences the phase behaviour of membranes [9,46]. Hydroxylation of sphingolipids could increase the stability of membranes by strengthening the lateral interactions of lipids and/or proteins [8,9]. Sphingolipids are important constituents of specialized membrane microdomains or rafts, which are important for intracellular trafficking, sorting and signal transduction [4]. It is possible that α-hydroxylation influences the formation of rafts or affects lipid raft function.

HFA-sphingolipids (HFA-GalC and HFA-sulphatide) are especially abundant in myelin, specialized plasma membranes of oligodendrocytes wrapped around axons to enable fast conduction of nerve impulses by saltatory conduction [36]. We show here that FA2H is expressed in the white matter of the brain and that its expression is up-regulated during the active phase of myelination between 1 and 3 weeks of age. The time course of its expression and its *in situ* hybridization pattern were very similar to those of other myelin-specific genes [30,33,34] and PLP respectively. These results strongly suggest that FA2H is responsible for fatty acid α-hydroxylation in oligodendrocytes and that α-hydroxylation is mainly regulated at the transcriptional level.

Only a few indirect indications of a functional role for α-hydroxylated sphingolipids in myelin are currently available. Mice lacking the GalC-synthesizing enzyme CGT have significantly reduced HFA-sphingolipid levels [47,48]. These mice have lower nerve conduction velocities and exhibit deficits in myelin structure and a progressive demyelination [47–49]. Recent observations in our laboratory showed that transgenic mice with decreased HFA-GalC content develop unstable myelin and demyelinate (S. N. Fewou, H. Büssow, V. Gieselmann and M. Eckhardt, unpublished work). The formation of a functional myelin sheath, however, does not necessarily depend on α-hydroxylated sphingolipids since myelin can be formed in urodeles (newts and salamanders) in the absence of α-hydroxylated sphingolipids [7]. Interestingly, in urodeles, there is no correlation between axonal diameter and myelin thickness, in contrast with mammals [7]. Furthermore, urodeles have a lower signal conduction velocity [7]. Whether this is only a coincidence or whether α-hydroxylated

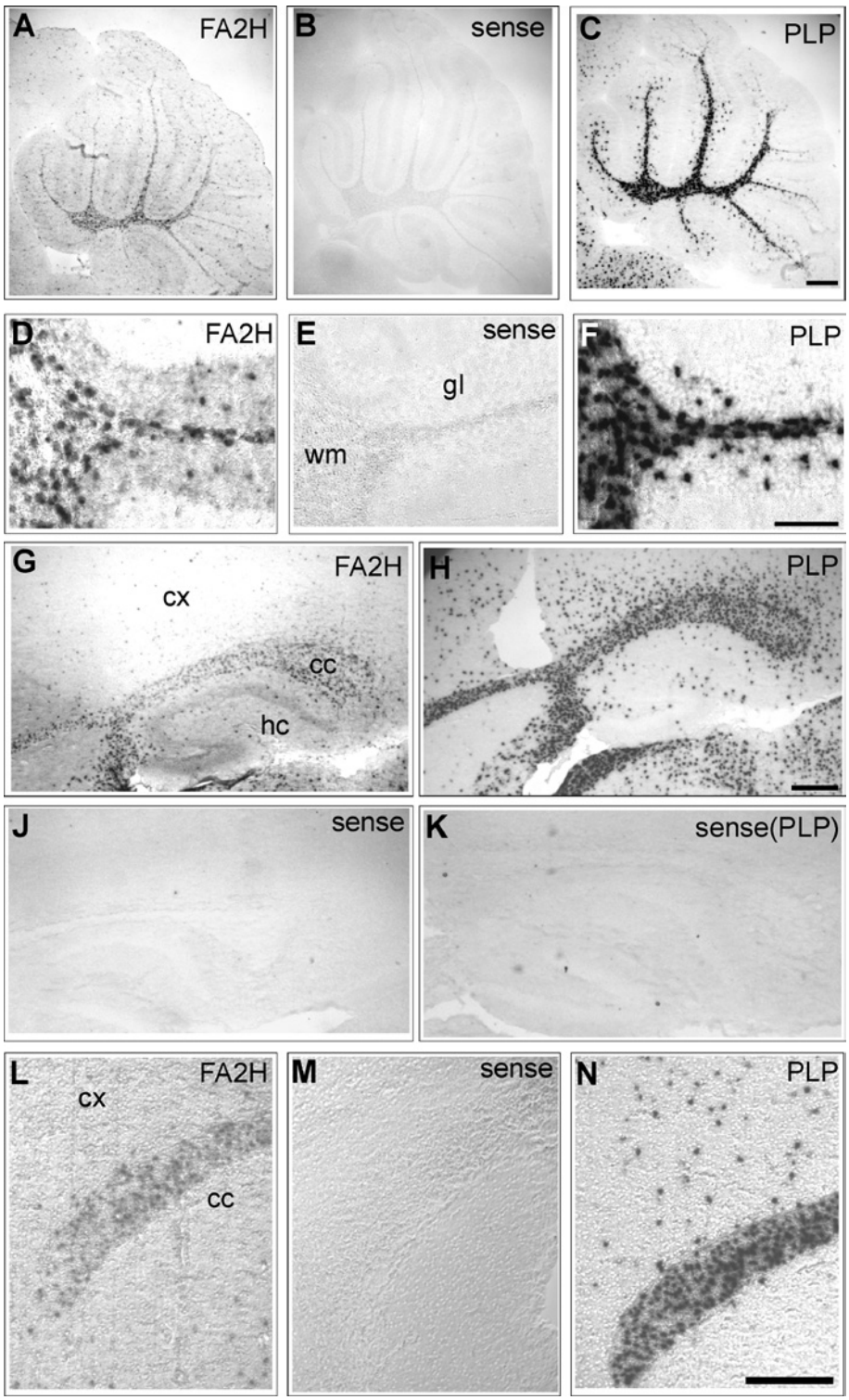

Figure 6 ***In situ*** **hybridization of 3-week-old mouse brains for FA2H mRNA**

Parasagittal sections of 3-week-old mouse brains were hybridized to DIG-labelled antisense FA2H (**A**, **D**, **G**, **L**) and PLP RNA probes (**C**, **F**, **H**, **N**). Control hybridizations with sense FA2H (**B**, **E**, **J**) and sense PLP RNA probes (**K**) gave no signals. Shown are the hybridization signals in cerebellum (**A**–**F**) and forebrain (**G**–**N**). Note the strong co-localization in the white matter of FA2H and PLP signals, suggesting FA2H expression in oligodendrocytes. cx, cortex; cc, corpus callosum; gl, granular layer; hc, hippocampus; wm, white matter. Scale bar, 200 μm (**A**–**C**, **G**–**N**) and 100 μm (**D**–**F**).

cerebrosides are required for the higher conduction velocity and to adjust myelin thickness to the axon diameter in higher vertebrates, will be answered in the future as soon as FA2H-deficient mice are available.

After submission of this paper, Alderson et al. [50] reported on the cloning of the human FA2H gene and showed that long chain fatty acids are substrates for the enzyme, although they did not test other potential substrates, e.g. ceramide.

We thank I. Ackermann for expert technical assistance and S. Schroeder for assistance with MALDI–TOF measurements. This study was supported by grants from the Deutsche Forschungsgemeinschaft to M.E. and V.G.

REFERENCES

1 Holthuis, J. C., Pomorski, T., Raggers, R. J., Sprong, H. and Van Meer, G. (2001) The organizing potential of sphingolipids in intracellular membrane transport. Physiol. Rev. **81**, 1689–1723

2 Obeid, L. M., Okamoto, Y. and Mao, C. (2002) Yeast sphingolipids: metabolism and biology. Biochim. Biophys. Acta **1585**, 163–171

3 Sperling, P. and Heinz, E. (2003) Plant sphingolipids: structural diversity, biosynthesis, first genes and functions. Biochim. Biophys. Acta **1632**, 1–15

4 Degroote, S., Wolthoorn, J. and Van Meer, G. (2004) The cell biology of glycosphingolipids. Semin. Cell Dev. Biol. **15**, 375–387

5 Sandhoff, K. and Kolter, T. (2003) Biosynthesis and degradation of mammalian glycosphingolipids. Philos. Trans. R. Soc. London B Biol. Sci. **358**, 847–861

6 Singh, I. and Kishimoto, Y. (1979) Alpha hydroxylation of lignoceric acid in brain. Subcellular localization of alpha hydroxylation and the requirement for heat-stable and heat-labile factors and sphingosine. J. Biol. Chem. **254**, 7698–7704

7 Kishimoto, Y. (1986) Phylogenetic development of myelin glycosphingolipids. Chem. Phys. Lipids **42**, 117–128

8 Graf, K., Baltes, H., Ahrens, H., Helm, C. A. and Husted, C. A. (2002) Structure of hydroxylated galactocerebrosides from myelin at the air-water interface. Biophys. J. **82**, 896–907

9 Koshy, K. M., Wang, J. and Boggs, J. M. (1999) Divalent cation-mediated interaction between cerebroside sulfate and cerebrosides: an investigation of the effect of structural variations of lipids by electrospray ionization mass spectrometry. Biophys. J. **77**, 306–318

10 Karlsson, K. A., Samuelsson, B. E. and Steen, G. O. (1973) The sphingolipid composition of bovine kidney cortex, medulla and papilla. Biochim. Biophys. Acta **316**, 317–335

11 Karlsson, K., Nilsson, K., Samuelsson, B. E. and Steen, G. O. (1969) The presence of hydroxy fatty acids in sphingomyelins of bovine rennet stomach. Biochim. Biophys. Acta **176**, 660–663

12 Madison, K. C. (2003) Barrier function of the skin: 'la raison d'etre' of the epidermis. J. Invest. Dermatol. **121**, 231–241

13 Takagi, S., Tojo, H., Tomita, S., Sano, S., Itami, S., Hara, M., Inoue, S., Horie, K., Kondoh, G., Hosokawa, K. et al. (2003) Alteration of the 4-sphingenine scaffolds of ceramides in keratinocyte-specific Arnt-deficient mice affects skin barrier function. J. Clin. Invest. **112**, 1372–1382

14 Motta, S., Monti, M., Sesana, S., Caputo, R., Carelli, S. and Ghidoni, R. (1993) Ceramide composition of the psoriatic scale. Biochim. Biophys. Acta **1182**, 147–151

15 Dunn, T. M., Haak, D., Monaghan, E. and Beeler, T. J. (1998) Synthesis of monohydroxylated inositolphosphorylceramide (IPC-C) in *Saccharomyces cerevisiae* requires Scs7p, a protein with both a cytochrome b5-like domain and a hydroxylase/desaturase domain. Yeast **14**, 311–321

16 Haak, D., Gable, K., Beeler, T. and Dunn, T. (1997) Hydroxylation of *Saccharomyces cerevisiae* ceramides requires Sur2p and Scs7p. J. Biol. Chem. **272**, 29704–29710

17 Eckhardt, M., Barth, H., Blöcker, D. and Aktories, K. (2000) Binding of *Clostridium botulinum* C2 toxin to asparagine-linked complex and hybrid carbohydrates. J. Biol. Chem. **275**, 2328–2334

18 Krogh, A., Larsson, B., von Heijne, G. and Sonnhammer, E. L. L. (2001) Predicting transmembrane protein topology with a hidden Markov model: application to complete genomes. J. Mol. Biol. **305**, 567–580

19 Kyte, J. and Doolittle, R. F. (1982) A simple method for displaying the hydropathic character of a protein. J. Mol. Biol. **157**, 105–132

20 Sambrook, J., Fritsch, E. F. and Maniatis, T. (1989) Molecular Cloning: A Laboratory Manual, 2nd edn, Cold Spring Harbor Laboratory Press, Plainview, NY

21 van Echten-Deckert, G. (2000) Sphingolipid extraction and analysis by thin-layer chromatography. Methods Enzymol. **312**, 64–79

22 Yao, J. K. and Rastetter, G. M. (1985) Microanalysis of complex tissue lipids by high-performance thin-layer chromatography. Anal. Biochem. **150**, 111–116

23 Bertello, L. E., Goncalvez, M. F., Colli, W. and de Lederkremer, R. M. (1995) Structural analysis of inositol phospholipids from *Trypanosoma cruzi* epimastigote forms. Biochem. J. **310**, 255–261

24 Baader, S. L., Sanlioglu, S., Berrebi, A. S., Parker-Thornburg, J. and Oberdick, J. (1998) Ectopic overexpression of engrailed-2 in cerebellar Purkinje cells causes restricted cell loss and retarded external germinal layer development at lobule junctions. J. Neurosci. **18**, 1763–1773

25 Fox, B. G., Shanklin, J., Somerville, C. and Munck, E. (1993) Stearoyl-acyl carrier protein delta 9 desaturase from *Ricinus communis* is a diiron-oxo protein. Proc. Natl. Acad. Sci. U.S.A. **90**, 2486–2490

26 Ternes, P., Franke, S., Zähringer, U., Sperling, P. and Heinz, E. (2002) Identification and characterization of a sphingolipid delta 4-desaturase family. J. Biol. Chem. **277**, 25512–25518

27 Fox, B. G., Shanklin, J., Ai, J., Loehr, T. M. and Sanders-Loehr, J. (1994) Resonance Raman evidence for an Fe-O-Fe center in stearoyl-ACP desaturase. Primary sequence identity with other diiron-oxo proteins. Biochemistry **33**, 12776–12786

28 Stahl, N., Jurevics, H., Moreli, P., Suzuki, K. and Popko, B. (1994) Isolation, characterization, and expression of cDNA clones that encode rat UDP-galactose:ceramide galactosyltransferase. J. Neurosci. Res. **38**, 234–242

29 van der Bijl, P., Strous, G. J., Lopes-Cardozo, M., Thomas-Oates, J. and van Meer, G. (1996) Synthesis of non-hydroxy-galactosylceramides and galactosyldiglycerides by hydroxy-ceramide galactosyltransferase. Biochem. J. **317**, 589–597

30 Schaeren-Wiemers, N., van der Bijl, P. and Schwab, M. E. (1995) The UDP-galactose:ceramide galactosyltransferase: expression pattern in oligodendrocytes and Schwann cells during myelination and substrate preference for hydroxyceramide. J. Neurochem. **65**, 2267–2278

31 Burger, K. N., van der Bijl, P. and van Meer, G. (1986) Topology of sphingolipid galactosyltransferases in ER and Golgi: transbilayer movement of monohexosyl sphingolipids is required for higher glycosphingolipid biosynthesis. J. Cell Biol. **133**, 15–28

32 Robinson, B. S., Johnson, D. W. and Poulos, A. (1992) Novel molecular species of sphingomyelin containing 2-hydroxylated polyenoic very-long-chain fatty acids in mammalian testes and spermatozoa. J. Biol. Chem. **267**, 1746–1751

33 Carson, J. H., Neilson, M. L. and Barbarese, E. (1983) Developmental regulation of myelin basic protein expression in mouse brain. Dev. Biol. **96**, 485–492

34 Sorg, B. A., Smith, M. M. and Campagnoni, A. T. (1987) Developmental expression of the myelin proteolipid protein and basic protein mRNAs in normal and dysmyelinating mutant mice. J. Neurochem. **49**, 1146–1154

35 Murad, S. and Kishimoto, Y. (1975) Alpha hydroxylation of lignoceric acid to cerebronic acid during brain development. Diminished hydroxylase activity in myelin-deficient mouse mutants. J. Biol. Chem. **250**, 5841–5846

36 Baumann, N. and Pham-Dinh, D. (2001) Biology of oligodendrocyte and myelin in the mammalian central nervous system. Physiol. Rev. **81**, 871–927

37 Shanklin, J., Whittle, E. and Fox, B. G. (1994) Eight histidine residues are catalytically essential in a membrane-associated iron enzyme, stearoyl-CoA desaturase, and are conserved in alkane hydroxylase and xylene monooxygenase. Biochemistry **33**, 12787–12794

38 Mizutani, Y., Kihara, A. and Igarashi, Y. (2004) Identification of the human sphingolipid C4-hydroxylase, hDES2, and its up-regulation during keratinocyte differentiation. FEBS Lett. **563**, 93–97

39 Mitchell, A. G. and Martin, C. E. (1997) Fah1p, a *Saccharomyces cerevisiae* cytochrome b5 fusion protein, and its *Arabidopsis thaliana* homolog that lacks the cytochrome b5 domain both function in the alpha-hydroxylation of sphingolipid-associated very long chain fatty acids. J. Biol. Chem. **272**, 28281–28288

40 Akanuma, H. and Kishimoto, Y. (1979) Synthesis of ceramides and cerebrosides containing both alpha-hydroxy and nonhydroxy fatty acids from lignoceroyl-CoA by rat brain microsomes. J. Biol. Chem. **254**, 1050–1060

41 Kaya, K., Ramesha, C. S. and Thompson, G. A. (1984) On the formation of alpha-hydroxy fatty acids. Evidence for a direct hydroxylation of nonhydroxy fatty acid-containing sphingolipids. J. Biol. Chem. **259**, 3548–3553

42 Svennerholm, L., Bostrom, K., Fredman, P., Jungbjer, B., Mansson, J. E. and Rynmark, B. M. (1992) Membrane lipids of human peripheral nerve and spinal cord. Biochim. Biophys. Acta **1128**, 1–7

43 Nakakuma, H., Arai, M., Kawaguchi, T., Horikawa, K., Hidaka, M., Sakamoto, K., Iwamori, M., Nagai, Y. and Takatsuki, K. (1989) Monoclonal antibody to galactosylceramide: discrimination of structural difference in the ceramide moiety. FEBS Lett. **258**, 230–232

44 Binnington, B., Lingwood, D., Nutikka, A. and Lingwood, C. A. (2002) Effect of globotriaosyl ceramide fatty acid alpha-hydroxylation on the binding by verotoxin 1 and verotoxin 2. Neurochem. Res. **27**, 807–813

45 Boggs, J. M., Menikh, A. and Rangaraj, G. (2000) Trans interactions between galactosylceramide and cerebroside sulfate across apposed bilayers. Biophys. J. **78**, 874–885

46 Shah, J., Atienza, J. M., Rawlings, A. V. and Shipley, G. G. (1995) Physical properties of ceramides: effect of fatty acid hydroxylation. J. Lipid Res. **36**, 1945–1955

47 Coetzee, T., Fujita, N., Dupree, J., Shi, R., Blight, A., Suzuki, K., Suzuki, K. and Popko, B. (1996) Myelination in the absence of galactocerebroside and sulfatide: normal structure with abnormal function and regional instability. Cell (Cambridge, Mass.) **86**, 209–219

48 Bosio, A., Binczek, E. and Stoffel, W. (1996) Functional breakdown of the lipid bilayer of the myelin membrane in central and peripheral nervous system by disrupted galactocerebroside synthesis. Proc. Natl. Acad. Sci. U.S.A. **93**, 13280–13285

49 Coetzee, T., Dupree, J. L. and Popko, B. (1998) Demyelination and altered expression of myelin-associated glycoprotein isoforms in the central nervous system of galactolipid-deficient mice. J. Neurosci. Res. **54**, 613–622

50 Alderson, N. L., Rembiesa, B. M., Walla, M. D., Bielawska, A., Bielawski, J. and Hama, H. (2004) The human FA2H gene encodes a fatty acid 2-hydroxylase. J. Biol. Chem. **279**, 48562–48568

Received 25 August 2004/20 December 2004; accepted 17 January 2005
Published as BJ Immediate Publication 20 January 2005, DOI 10.1042/BJ20041451